Heterogeneity of the Japanese islands as inferred from transverse component analyses of teleseismic *P*-waves observed at a seismic station network, Hi-net

Takeshi Nishimura

Department of Geophysics, Graduate School of Science, Tohoku University, 6-3 Aramaki-aza Aoba, Aoba-ku, Sendai 980-8578, Japan

(Received November 16, 2011; Revised October 1, 2012; Accepted October 5, 2012; Online published November 1, 2012)

Teleseismic *P*-waves are observed even in a transverse component, and the ratio of the peak energy of the transverse component to that of the sum of the three components (peak energy ratio) is a good indicator to represent the strength of the heterogeneity in the structure. We analyze the short-period teleseismic *P*-waves recorded at a dense seismic network in Japan (Hi-Net) and determine the spatial changes of the heterogeneity in the Japanese islands. The results show that east Japan is characterized mainly by large peak energy ratios that represent strong heterogeneity. On the other hand, west Japan shows small peak energy ratios. Comparison of the results with detailed geological maps further shows that large peak energy ratios are observed at regions located close to both quaternary volcanoes and active faults, and the active fault region is characterized by slightly smaller peak energy ratios. Non-active regions, located far from volcanoes or faults, indicate the smallest ratios, although the ratios are larger than those estimated on stable continents. Plains that consist mainly of sediments show the largest peak energy ratios. However, peak delay times observed at the plains are much longer than the others, which suggests a different mechanism for generating the amplitudes in the transverse component.
Key words: Teleseismic *P*-wave, transverse component, heterogeneity, volcano, active fault plain.

1. Introduction

Recent analyses of short-period waves recorded by a dense seismic network (Hi-net) have succeeded in determining small-scale heterogeneities of the crust and lithosphere. Multi-lapse time window analyses for *S*-waves and their coda from local earthquakes clarified detailed spatial distributions of intrinsic and scattering Q of the crust in Japan (Carcore and Sato, 2009). Peak delay times of *S*-waves propagating in the medium characterized by von Kerman type spectrum of fluctuations are also used to evaluate the small-scale heterogeneity beneath the Tohoku region, Japan (Takahashi *et al*., 2009). Their spatial resolutions are high enough to compare the elastic parameters related with the small-scale heterogeneity to the tectonic settings at the target regions, such as volcanoes, active seismic faults, and so on.

Energy partitioning of a teleseismic *P*-wave into a transverse component, which is perpendicular to the propagation direction on the ground surface, is also used to evaluate the heterogeneity in the lithosphere. This method has the merit in that we can evaluate the heterogeneity even at regions where local earthquakes are not observed. Large amplitudes are observed in the transverse component at stations located on active tectonic regions, while small amplitudes are observed on stable continents (Nishimura, 1996; Nishimura *et al*., 2002; Kubanza *et al*., 2006, 2007). Sato (2006) has formulated the vector waves of *P*-waves incident to the heterogeneity characterized by a Gaussian power spectrum of the fluctuation, and has shown that the peak energy ratio, which is the ratio of the maximum amplitude of the mean square envelope of the transverse component to that of the sum of the three components, is approximately equal to $1.81\epsilon^2 z/a$, where ϵ is the fractional change of seismic velocity, a is the correlation length and z is the thickness of the heterogeneous medium.

In the present study, we analyze teleseismic *P*-waves observed at a highly-dense seismic network, Hi-net, Japan, which deploys short-period seismometers with an average spacing of a few tens of kilometers. Comparing the geological settings in Japan, we quantify the small-scale heterogeneity and discuss the origins that produce amplitudes in the transverse component of the *P*-wave.

2. Data and Analyses

We analyze about 90 deep earthquakes with a source depth of more than 300 km to avoid contaminations of depth phases in the *P*-coda. The earthquakes analyzed in the present study are observed for the period from 2005 to 2009, and their magnitudes range from 5.5 to 6.5. The epicentral distances are 0.013 to 84 degrees, and the back azimuth mostly distribute in the north-east or south directions. Peak energy ratios are measured by the same procedure used in Kubanza *et al*. (2007). We first correct the response of the seismometers, band-pass filter the data at the frequency bands of 0.5–1, 1–2, 2–4, and 4–8 Hz, and calculate the transverse component from the two horizontal components for each earthquake based on the locations of station and epicenter. Then, stacking the squared velocity seismograms of different earthquakes at each station, we obtain

doi:10.5047/eps.2012.10.001

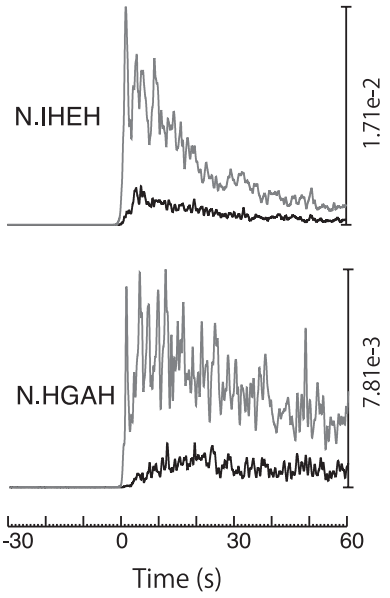

Fig. 1. Examples of the mean square envelopes of transverse components (black lines) and the sum of the three components (gray lines) at 1–2 Hz. (a) N.IHEH station that is located close to Iwate and Hachiman-tai volcanoes; (b) N.HGAH station on the Kanto plain.

the mean squared envelope of the transverse component as well as that of the sum of the three components. No time window is used for stacking the data. Figure 1 shows examples of the mean squared envelopes observed at two stations characterized by different geological features: N.IHEH station is located close to quaternary volcanoes, and N.HGAH station is on the Kanto plain. The peak energy ratios are measured by taking the ratio of the maximum amplitude of the mean squared envelope of the transverse component to that of the sum of the three components. We show the results for stations having more than eight *P*-wave data with a maximum amplitude 10 times larger than the noise signals.

3. Results

Hi-net stations are densely distributed on the Japanese islands, so, in Fig. 2, we plot the peak energy ratio measured at each station. Results of the peak energy ratio at the four frequency bands are shown. The spatial distributions are almost similar to each other, although the peak energy ratios tend to increase with frequency.

We summarize the basic characteristics of the spatial distributions of the peak energy ratios with reference to the geological setting of the Japanese islands. Figure 3 shows the active faults taken from the digital map edited by Nakata and Imaizumi (2002), and the quaternary volcanoes from Committee for Catalog of Quaternary Volcanoes in Japan (1999). We define 'plains' for the regions classified as loam plain, natural levee, back slough, old river channel, delta and bar in Wakamatsu *et al*. (2005), and plot them in Fig. 3. Firstly, it is found that the Japanese islands are divided mainly into two regions at a boundary in the Chubu region: large peak energy ratios in east Japan and small ones in west Japan. Even in west Japan, however, it is found that regions close to volcanoes show peak energy ratios larger than the surroundings; for instance, the central part of the Kyushu region and the northern part of the Chugoku region. The Tohoku region, where a volcanic front extends in the north-south direction, shows large ratios, but small ratios are also recognized in regions along the east coast. Large peak energy ratios are recognized around Tokyo on the Kanto plain. In west Japan, slightly-large peak energy ratios are seen on the middle of the Shikoku region, where the median tectonic line crosses. In spite of a large number of active seismic faults (Working Group for Compilation of 1:2,000,000 Active Faults Map of Japan, 2000), the regions from central Japan to the Kinki region are characterized by small peak energy ratios.

To investigate systematically the origins of heterogeneity that produce transverse energy in a *P*-wave, we classify the Japanese islands into the following five regions by using the digital map shown in Fig. 3: (i) the active fault regions that are within a distance of 20 km from an active fault, or an estimated active fault which is not directly observed on the ground surface but is inferred from topography, (ii) volcano regions that are within a distance of 20 km from a quaternary volcano, (iii) the plains, as defined above, which are characterized by sediments, (iv) the volcano and fault regions that are within a distance of 20 km both from a quaternary volcano and an active fault, and (v) regions that are more than 20 km removed from volcanoes and faults, and which are not located on a plain (we refer to these as 'non-active regions'). The five regions do not overlap: each of the regions of (i)–(iii) contains only one of volcano, fault or plain, (iv) includes both volcano and fault, and (v) includes none of them.

We examine the peak energy ratios at the four frequency bands for all of the data and the five regions, and obtain the averages with 95% confidence levels and standard deviations of the peak energy ratios (Table 1). The largest average peak energy ratio is found for the plain regions at each frequency band (the averages are 0.19–0.25). The volcano and fault regions also show large average peak energy ratios (0.16–0.23). The smallest average peak energy ratio is found for the non-active regions (0.10–0.15). The ratio is still larger than those obtained for the global data that are observed at stations located on the stable continents and island arcs (0.04 at 0.5–1 Hz, 0.087 at 1–2 Hz, and 0.141 at 2–4 Hz; Kubanza *et al*., 2007), which implies that the Japanese islands are much more heterogeneous than the stable continents, even in the case of regions without active faults and volcanoes. The estimated standard deviations are as large as the averages. Hence, we apply Student's t-test to examine whether, or not, the averages at the regions (i), (iv) and (v) are statistically different from each other, although (i) and (v) for 2–4 Hz is different at the 75 % confidence level. We do not discuss (ii) volcano regions and (iii) plains because the number of data is small. The results show that these three regions are significantly different from each other at the 95 % confidence level.

From the average peak energy ratios shown in Table 1 (about 0.1–0.2) and Sato (2006), we estimate the quantity ϵ^2/a to be about 5.5×10^{-4}–1.1×10^{-3} km^{-1} for tentatively assuming the thickness of heterogeneity $z = 100$ km. The fluctuation ϵ ranges 5 to 7% for $a = 5$ km.

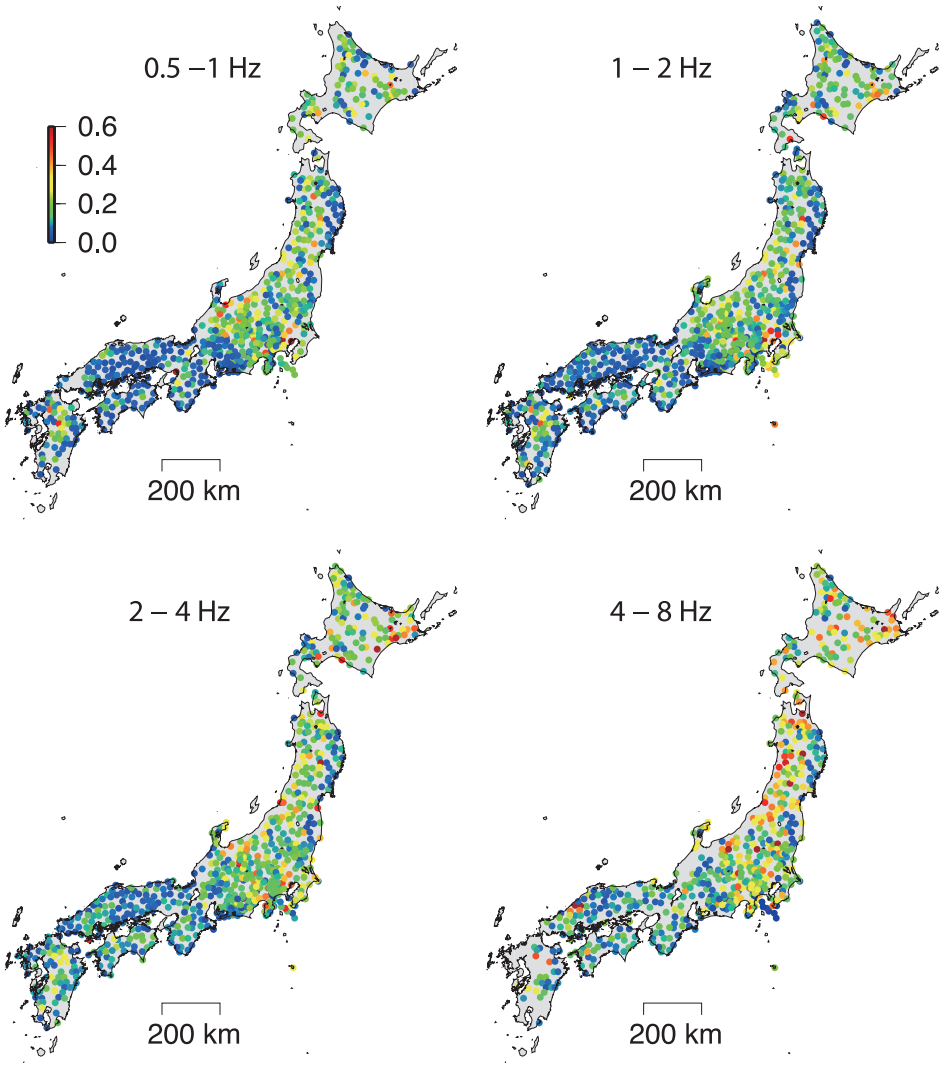

Fig. 2. Spatial variations of the peak energy ratio in the Japanese islands at the four frequency bands.

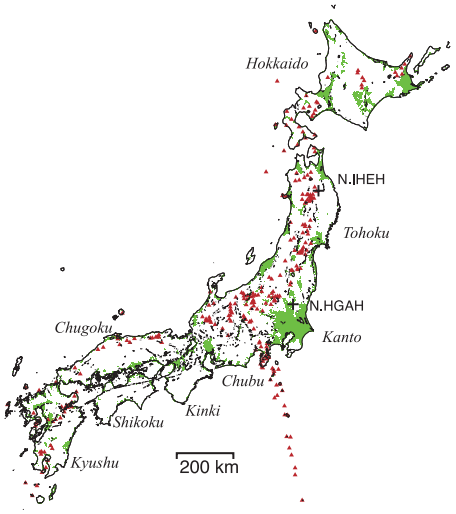

Fig. 3. Distributions of geological features in the Japanese islands. Brown triangles: quaternary volcanoes (Committee for Catalog of Quaternary Volcanoes in Japan, 1999). Solid lines: active faults and estimated active faults (Nakata and Imaizumi, 2002). Green colors: plains defined as loam plain, natural levee, back slough, old river channel, delta and bar in Wakamatsu *et al*. (2005). The plus symbols represent stations N.IHEH and N.HGAH of Fig. 1.

4. Discussion

Spatial distributions of the peak energy ratios (Fig. 2) are not well correlated with three-dimensional *P*- or *S*-wave velocity distributions (e.g., Matsubara *et al*., 2008). For example, a drastic change from east to west Japan is not recognized in the *P*- and *S*-wave velocity distributions. Carcole and Sato (2009) have determined intrinsic absorption Q_i^{-1} and scattering loss Q_s^{-1} values in the Japanese islands from multi-lapse time window analyses. Spatial distributions of the scattering loss obtained at 1–2 and 2–4 Hz are similar to those of the peak energy ratios. For example, large values of scattering loss are found in east Japan and in the middle of Kyushu, while small values are found in west Japan and along the Sanriku coast. This consistency strongly suggests that the peak energy ratios represent the strength of scattering in the structure, although the results at 4–8 Hz show some differences in the spatial distributions: for example, a large scattering loss in west Japan from Chugoku to central Japan.

We further examine the peak delay time that is the time lag from *P*-wave onset to the maximum amplitude, and summarize these in Table 1. The peak delay times are measured for the mean square envelopes both of the transverse

Table 1. Averages and the 95% confidence level of peak energy ratios and peak delay times.

Freq. (Hz)	Peak Energy Ratio	Peak Delay Time (s) 3 comp.	Trans.	N
		All data		
0.5-1	0.14±0.01(0.11)	3.7±0.3 (3.9)	10.7±0.5(6.7)	635
1-2	0.14±0.01 (0.10)	3.1±0.2 (3.2)	8.6±0.4 (5.2)	725
2-4	0.16±0.01 (0.11)	3.2±0.3 (3.3)	7.0±0.3 (4.7)	712
4-8	0.20±0.01 (0.14)	3.4±0.3 (3.2)	6.5±0.4 (4.6)	574
		Active Fault		
0.5-1	0.12±0.01 (0.11)	3.2±0.3 (3.0)	10.4±0.7 (6.7)	266
1-2	0.13±0.01 (0.10)	2.8±0.3 (3.1)	8.4±0.6 (5.1)	297
2-4	0.15±0.01 (0.10)	2.8±0.4 (3.1)	6.9±0.6 (4.8)	294
4-8	0.19±0.02 (0.13)	3.2±0.4 (2.8)	6.4±0.6 (4.4)	240
		Quaternary Volcano		
0.5-1	0.16±0.03 (0.09)	4.3±1.4 (3.8)	9.2±1.5 (4.4)	30
1-2	0.14±0.03 (0.08)	3.5±1.1 (3.4)	7.3±1.4 (4.1)	37
2-4	0.17±0.03 (0.08)	3.1±0.9 (2.7)	5.9±1.2 (3.7)	36
4-8	0.24±0.06 (0.15)	4.0±1.4 (3.7)	5.5±1.4 (3.8)	29
		Plain		
0.5-1	0.20±0.09 (0.18)	7.4±2.9 (7.0)	14.1±3.8 (17)	17
1-2	0.19±0.05 (0.13)	4.7±1.5 (4.3)	13.4±2.9 (6.6)	25
2-4	0.24±0.05 (0.12)	5.4±2.1 (4.7)	12.3±2.0 (5.0)	24
4-8	0.25±0.06 (0.14)	4.5±1.4 (2.7)	9.2±1.9 (4.2)	21
		Quaternary Volcano & Active Fault		
0.5-1	0.18±0.02 (0.10)	4.2±0.6 (4.0)	10.5±0.9 (5.9)	172
1-2	0.16±0.01 (0.09)	3.2±0.4 (2.5)	8.1±0.7 (4.6)	188
2-4	0.19±0.02 (0.11)	3.5±0.4 (3.0)	6.4±0.6 (3.9)	183
4-8	0.23±0.02 (0.13)	3.5±0.4 (2.8)	6.0±0.7 (4.3)	149
		Non-Active Region		
0.5-1	0.10±0.01 (0.08)	3.4±0.7 (3.7)	11.5±1.3 (7.0)	121
1-2	0.11±0.02 (0.09)	2.9±0.6 (3.7)	8.4±0.8 (5.2)	137
2-4	0.14±0.02 (0.11)	2.9±0.6 (3.7)	6.8±0.7 (4.1)	136
4-8	0.15±0.02 (0.11)	3.0±0.7 (3.8)	6.5±0.9 (4.7)	111

* N is the number of stations used. 3 comp means the sum of three components. Numeral in bracket represents one standard deviation.

component and for the sum of the three components. It is clearly recognized that the peak delay times for the plains are longer than those for the other regions: the peak delay times for the sum of three components are about 4–7 s for the plain and 3–4 s for the others, and those for the transverse component are 9–14 s for the plain, while about 6–11 s for the others. Observed long peak delay times are probably due to the differences in the mechanisms generating the seismic amplitudes in the transverse component. Conversion phases or surface waves generated by the sedimentary layers are considered to be the origins of the transverse component in teleseismic P-waves observed at the plains.

Sato (2006) relates peak delay times with the heterogeneous media by $t_p^{\rm sum} = 0.67 t_M$ for the sum of the three components and $t_p^{\rm trn} = 1.63 t_M$ for the transverse component, where $t_M = \sqrt{\pi}\epsilon^2 z^2/(2V_p a)$ and V_p is the P-wave velocity. The peak delay times predicted from the observed peak energy ratio (0.09–0.24) for the regions except the plain are estimated to be less than about 2 s for $z = 100$ km and $V_p = 6$ km/s. This estimated value (<2 s) is much shorter than the observations. Also, the peak delay times do not seem to increase with the peak energy ratios, although Sato's (2006) model predicts a positive correlation between the two parameters. This is probably because source duration times of earthquakes with magnitudes of 5.5–6.5 are a few seconds or more, and we stack envelopes of different earthquakes.

Acknowledgments. This study is greatly indebted to the data of high sensitivity seismograph network (Hi-net) by the National Research Institute for Earth Science and Disaster Prevention (NIED), Japan. Careful comments by two anonymous reviewers improved this manuscript. This study is partly supported by the Ministry of Education, Culture, Sports, Science and Technology in Japan MEXT (No. 20540405).

References

Carcole, E. and H. Sato, Spatial distribution of scattering loss and intrinsic absorption of short-period S waves in the lithosphere of Japan on the basis of the Multiple Lapse Time Window Analysis of Hi-net data, *Geophys. J. Int.*, **180**, 268–290, 2009.

Committee for Catalog of Quaternary Volcanoes in Japan, Catalog of Quatenary volcanoes in Japan, *Bull. Volcanol. Soc. Jpn.*, **44**, 285–289, 1999.

Kubanza, M., T. Nishimura, and H. Sato, Spatial variation of lithospheric heterogeneity on the globe as revealed from transverse amplitudes of short-period teleseismic P-waves, *Earth Planets Space*, **58**, e45–e48, 2006.

Kubanza, M., T. Nishimura, and H. Sato, Evaluation of strength of heterogeneity in the lithosphere from peak amplitude analyses of teleseismic short-period vector P-waves, *Geophys. J. Int.*, **171**, 390–398, 2007.

Matsubara, M., K. Obara, and K. Kasahara, Three-dimensional P- and S-wave velocity structures beneath the Japan Islands obtained by high-density seismic stations by seismic tomography, *Tectonophysics*, **454**, 86–103, 2008.

Nakata, T. and T. Imaizumi (eds), *Digital Active Fault Map of Japan*, 60 pp., Univ. Tokyo Press, 2002.

Nishimura, T., Horizontal layered structure with heterogeneity beneath continents and island arcs from particle orbits of long-period P waves, *Geophys. J. Int.*, **127**, 773–782, 1996.

Nishimura, T., K. Yoshimoto, T. Ohtaki, K. Kanjo, and I. Purwana, Spatial distribution of lateral heterogeneity in the upper mantle around the western Pacific region as inferred from analysis of transverse components of teleseismic P-coda, *Geophys. Res. Lett.*, **29**, doi:10.1029/2002GL015606, 2002.

Sato, H., Synthesis of vector-wave envelopes in 3-D random elastic media characterized by a Gaussian autocorrelation function based on the Markov approximation I: plane wave case, *J. Geophys. Res.*, **111**, doi:10.1029/2005JB004036, 2006.

Takahashi, T., H. Sato, T. Nishimura, and K. Obara, Strong inhomogeneity beneath Quaternary volcanoes revealed from the peak delay analysis of S-wave seismograms of microearthquakes in northeastern, Japan, *Geophys. J. Int.*, **168**, 90–99, doi:10.1111/j.1365-246X.2006.03197.x., 2009.

Wakamatsu, K., S. Kubo, M. Matsuoka, K. Hasegawa, and M. Sugiura, *Japan Engineering Geomorphologic Classification Map*, 104 pp, Univ. Tokyo Press, 2005.

Working Group for Compilation of 1:2,000,000 Active Faults Map of Japan, 1:2,000,000 active fault map of Japan, *Active Fault Res.*, **19**, 3–12, 2000.

T. Nishimura (e-mail: nishi@zisin.gp.tohoku.ac.jp)